Indonesian Journal of Electrical Engineering and Informatics (IJEEI)
Vol. 13, No. 3, September 2025, pp. 548~557
ISSN: 2089-3272, DOI: 10.52549/ijeei.v13i3.6747

Angularly Stable, Transparent and Flexible Modified Octagonal Shaped Frequency Selective Surface (FSS) for Sub-GHz 5G Applications

Gotte Ranjith Kumar[1], Swetha S[2], Deepan S[3], Loganathan AS[4], Muthu Manickam A[5] and Lavanya S[6]

[1]Assistant Professor, SR University, Warangal, Telangana, India.
[2]Assistant Professor, St. Joseph's Institute of Technology, Tamil Nadu, India.
[3]Assistant Professor, Vel Tech Rangarajan Dr. Sagunthala R&D Institute of Science and Technology, Tamil Nadu, India.
[4]Assistant Professor, Chennai Institute of Technology, Tamil Nadu, India.
[5]Assistant Professor, Shanmuganathan Engineering College, Tamil Nadu, India.
[6]Assistant Professor, Jerusalem College of Engineering, Tamil Nadu, India.

Article Info

Article history:

Received May 31, 2025
Revised Jun 22, 2025
Accepted Aug 10, 2025

Keywords:

Frequency Selective Surface (FSS)
Miniaturization
Angular Stability
Wideband
5G wireless communication

ABSTRACT

This paper offers a newly size-reduced Frequency Selective Surface (FSS) featuring band-stop behavior at 4.2 GHz. This developed FSS includes a mushroom-shaped arm with an octagonal patch. The patch is extensively adjusted by incorporating further mushroom-shaped arms, leading to a lower resonance and wider bandwidth. The designed FSS is made up of just a 11 × 11 mm unit cell on a flexible acrylic substrate that is 1 mm thick. The proposed FSS had a 1 GHz bandwidth with a centre resonance frequency of 4.2 GHz. Due to the distinct polarization behavior of this FSS, the Transverse Magnetic (TM) and Transverse Electric (TE) modes are unique and have a steady angular property up to 45º. Measurements of S-parameters for TE and TM polarizations have been validated experimentally over the 2–8 GHz frequency spectrum for both normal and oblique incident angles up to 45°. Excellent agreement between the measured and simulated data is demonstrated, verifying the FSS performance with a frequency variation of less than 3% and preserving constant band-stop properties across all measured orientations. It may be appropriate for incorporation into applicable clothes in a variety of areas because of its simplicity and ease of fabrication.

Corresponding Author:

Swetha. S
Assistant Professor
Department of ECE
St. Joseph's Institute of Technology
Chennai, Tamil Nadu, India 600119
swethasrdhr88@gmail.com

1. INTRODUCTION

Since their intriguing characteristics attracted a lot of attention, FSS designs are becoming more and more useful as wireless communication and manufacturing technologies progress. There are many common uses for FSS, particularly in the microwave and low-millimetre-wave sectors. Some of these uses include integrated filters, electrically scanning phased arrays, waveguides, antennas, GPS, mobile telephony, and Bluetooth connectivity [1]. Several developments in the microwave domain focus on direct management of electromagnetic power and distribution, such as reflections, electromagnetic windows, and radiation pattern adjustment.

In every antenna design, surface waves are undesirable. The efficiency and realized gain of the antennas decreased as a result of their propagation via the ground plane rather than in free space. A further effect of surface waves is the deterioration of antenna radiation patterns. Surface wave dispersion raises back lobe radiation, which lowers the SNR in wireless devices like GPS receivers. Surface waves become more prevalent as the value of the dielectric constant rises, as shown in RF circuits that employ materials with a large

dielectric constant [2,3]. Nowadays, bandpass filters are quite common because of the need for high-speed transmission of data. Surface waves cause spurious stop bands to develop, which deteriorates the filtering function [4]. SSN-induced resonance mode stimulation, which compromises signal integrity, is another concern with multilayered PCBs. The use of FSS structures can reduce or eliminate the issues with microwave circuits that have been mentioned above. Periodic metal patches on a dielectric substrate make up electromagnetic band gap structures. It is also possible to create FSS structures with just a mix of dielectrics. FSS structures have the ability to reflect any incoming wave without changing phase and to block surface waves from propagating in a specific frequency range. Improved antenna characteristics can be obtained by utilizing the aforementioned FSS structure qualities [5].

Among the most well-known techniques to enhance antenna performance, an FSS implemented on a flexible substrate has gained significant attention recently [6]. It could be of benefit to increase gain as well as quality factors and decrease the impact of the antenna's connection to a person's body because of its capability to block surface waves and produce no reflect phase. The Coplanar Waveguide (CPW) antenna's bandwidth, gain and ability to block backward radiation were presentsd to be enhanced by the FSS [7]. Furthermore, because of the multilayer study, there are mismatch problems because of the various components that need to be assembled, but the lateral dimension is still quite large [8].

Two distinct ways to employ FSS design to increase antenna gain are to use it as a ground plane [9] or as a superstrate [10]. Additionally, FSS is utilized in MIMO networks to enhance the isolation property and diversity gain [11]. FSS is also utilized in UWB antennas for obtaining notched characteristics [12]. FSSs are also employed in fast networks to reduce Interference and attenuate noises [13]. A selection of the FSS structures' mathematical investigations and models can be found in the references. Although the open literature presents numerous strategies for designing dual band and multiband FSS structures, the majority of these techniques have narrow or limited bandwidths [14-16].

Flexible and frequency-reconfigurable FSS achieves a broad tuning range of resonate from 3.5 to 5.7 GHz. The broad angle stability from 0° to 60°, another crucial characteristic for flexible or conformal FSS, has also been studied [17]. A fundamental resonance was obtained at 12.5 GHz from a circular FSS array printed on a thin polycarbonate film. Higher angles between 30° and 90° are shown to produce a 3.3% frequency shift [18]. A floating glass substrate with a surface incidence angle of as much as 80° in both TE and TM modes has been employed in an innovative geometric design for FSS that was anticipated to attain 70% transparency [19]. Another FSS has been built specifically for X-band applications, with a flexible and compact polymide substrate [20]. For planar and all conformal geometries, a steady angular response up to 60° is provided by an effective and miniature wideband polygon-shaped frequency selective surface (PFSS) [21]. Another FSS is described as being illuminated using an electromagnetic wave, with scattering parameters that remain stable under varying incidence angles as much as 80° for both TE and TM polarization [22]. An innovative dual-band enhanced Jerusalem stepped looped frequency-selective surface (FSS)-based electromagnetic shield application that is not affected by polarization. Its four-fold geometric uniformity allows for improved angular stability (up to ±75◦) and polarization insensitivity [23].

This study offers an innovative modified FSS having bandstop characteristics for 5G applications at a frequency of 4 GHz. The dimensions of the layout are 11 × 11 mm. At 4.2 GHz, the proposed FSS gives a band-stop response. The symmetric structure of the FSS meets polarization-independent characteristics. Furthermore, a constant frequency reaction for a range of angular occurrences is offered by the proposed FSS. For angles of the incident up to 30^0, the proposed FSS design offers superior stability capability and polarization-independent characteristics. The remaining portions have been arranged like this: The proposed design of the FSS unit cell is explained in Section II. The various steps of design for achieving the proposed FSS structure are covered in Section III. The scattering parameters, angle of incident, surface current analysis, and reflection phases of the FSS design are shown in Section IV. Section V concludes this investigation.

2. DESIGN METHODOLOGY

The modified octagonal radiating surface placed on a 1 mm thin flexible acrylic substrate layer makes up the unit cell of the proposed FSS configuration illustrated in Figure 1. The acrylic substrate possesses a dielectric value of 2.6 and loss tangent of 0.025. These values show an excellent balance of electrical functionality and affordability. The radiating patch is composed of mushroom-shaped patch with 8 arms that have been added, each with a thickness of 0.035 mm, and a modified octagonal patch. The intended FSS structure's total measurements are S = 11 mm, L1 = 2 mm, L2 = 2.6 mm, L3 = 1.6 mm, and D = 7.6 mm.

Figure 2 depicts the S-parameter values for the transmission coefficient (S_{11}) and reflection coefficient (S_{21}) of the proposed FSS, which are used to analyze its radiation properties. Bandstop response is shown in the transmission coefficient characteristics, and the bandpass response is seen in the reflection coefficient characteristics. With an insertion level of $S_{11} \leq$ -10 dB, the proposed FSS structure's band stop response offers an excellent bandwidth of 1 GHz from 3.61 GHz to 4.63 GHz at the centre frequency of 4.2 GHz. The FSS

structure offers greater bandwidth as well as associated transmission characteristics at the operational frequency. The proposed design offers a successful bandgap width of 25% and could successfully decrease transmission coefficients (S_{11}) in the stopband.

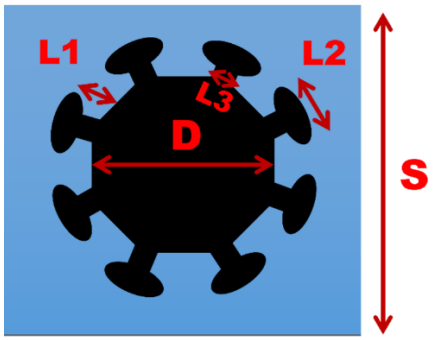

Figure 1. Detailed view of the proposed FSS design.

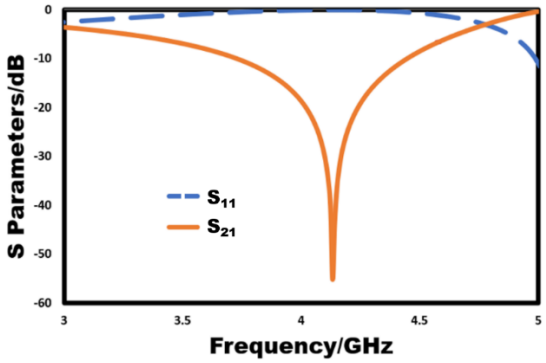

Figure 2. Simulated S-parameter of the proposed FSS design.

3. PARAMETRIC STUDY

The proposed FSS is developed and simulated with the widely used CST Studio software. Figure 3 illustrates the way the FSS design developed. The circular patch's initial diameter of 38.3 mm for fr = 3.6 GHz is selected. This FSS has a 180 MHz bandwidth and operates in the 3.61 GHz narrow-band frequency band in Iteration 1 has been given as Figure 3(a). The circular patch's circumference is where current distributions are most prominent. Adding another resonator increases the resonance and the octagonal patch's surface current distribution is disturbed. Iteration 2 has an achieved bandwidth of 0.65 GHz and a center frequency of 4.9 GHz is illustrated in Figure 3(b). Increasing the number of mushroom-shaped resonators is required to provide increased performance. The improved performance at 4.2 GHz is analyzed in the final Iteration 3 of the proposed FSS design is shown in Figure 3(c). Consequently, an excellent bandwidth performance of 1 GHz has been achieved in the design of the proposed FSS structure, and it also offers an identical response in both TM (Transverse Magnetic) and TE (Transverse Electric) modes.

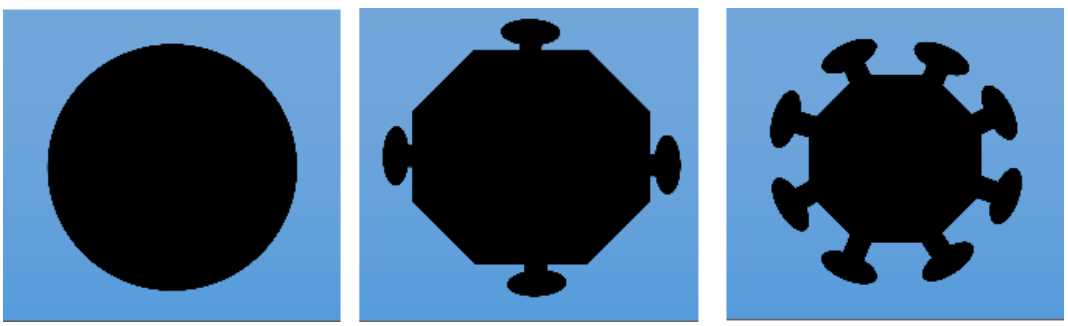

(a) (b) (c)

Figure. 3 Development stages of the proposed FSS design. (a) Iteration 1, (b) Iteration 2, and (c) Iteration 3.

4. RESULTS AND DISCUSSION

Determining the comparable circuit design is heavily reliant on the incident wave's polarization and the FSS structure's geometry. The distribution of the electric field and the current routes will determine the appearance of capacitances and inductances on the unit cell, respectively. Figure 4 depicts the relationship between capacitive and inductive elements, as well as the geometry of the structure and incident wave in a strip line, where L represents the strip inductance and C represents the capacitance between two neighboring arms. The incident mode and angle of incidence have a significant impact on the equivalent circuit and element values. Figure 4(a) shows the capacitive and inductive components of the FSS unit cell. Figure 4(b) displays the suggested FSS structure's simplified equivalent circuit.

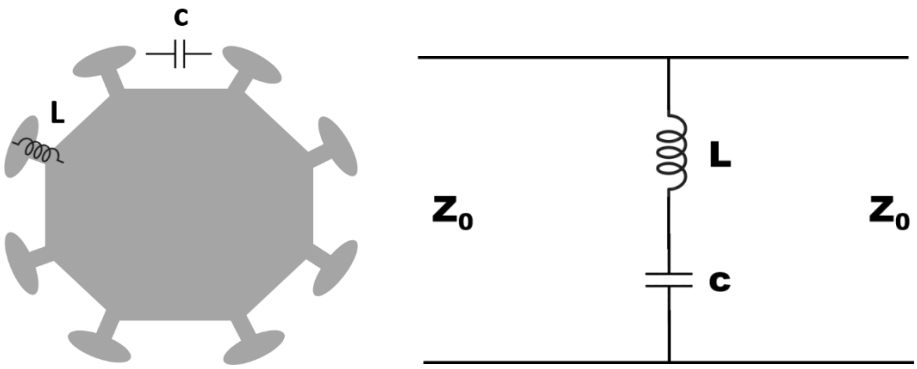

(a) (b)

Figure 4. Equivalent circuit of proposed FSS. (a) capacitive and inductive elements on FSS unit cell, and (b) Simplified form of equivalent circuit.

The FSS structure's connection to the wavenumber and resonant frequency is depicted in the dispersion diagram. Additionally, it may characterize the propagating modes and potential bandgaps between them, as well as the propagation features of an indefinitely periodic structure. The lower and higher bandgap frequencies are found by utilizing an Eigen mode solver to derive the FSS's dispersion parameters. It calculates the resonant frequencies for a given wave number based on the rectangular Brillouin zone. Figure 5 displays the dispersion diagram for the proposed FSS. The frequency range covered by the obtained band gap proposed FSS plane is 3.6 to 5.9 GHz.

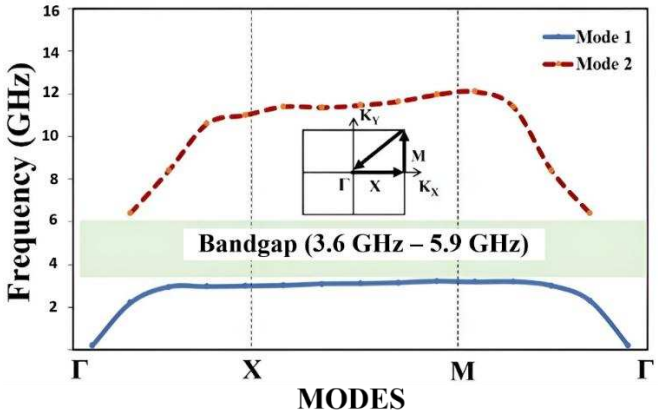

Figure 5. The obtained dispersion diagram of the proposed FSS structure.

The unit cell for the X- and Y-axes and open space for the Z-axis have been chosen as the boundary constraints of the FSS design. The symmetrical structure of the proposed design contributed in getting polarization-independent properties. The proposed layout ought to provide a comparable response at all incident angles. The stability of angle performances and a set of transmission parameters obtained using CST are shown in Figure 6.

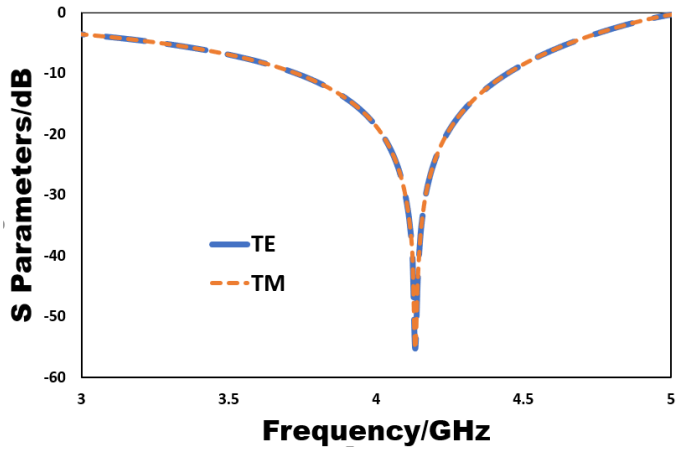

Figure 6. Stability response of the proposed FSS at both TE and TM modes.

According to the simulation results, a constant frequency response for both phi and theta values that range up to 30° is provided by the TE mode. The simulated FSS design of the TM mode is depicted in Figure 7, which has a similar frequency dependence for both theta and phi constants up to 45°. A steady frequency response was obtained at various incident angles in both the TE and TM mode setups of the proposed structure, which provided an effective bandwidth of 1GHz and a central frequency of 4.2 GHz shown in Figure 7(a) and 7(b), respectively. The poles and zero points of the transmission also remain relatively unchanged when the incoming electromagnetic radiation angle rises, irrespective of TE or TM polarization.

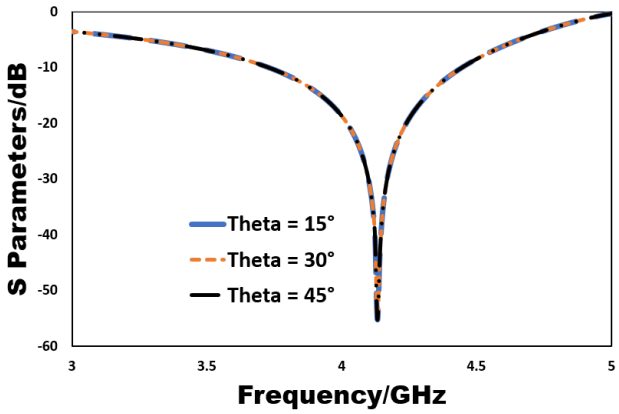

(a)

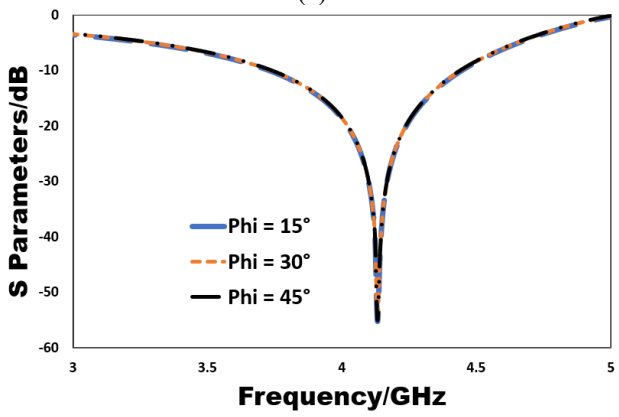

(b)

Figure 7. Stability response of the proposed FSS. (a) Theta orientation and (b) Phi orientation.

The proposed FSS structure's surface current patterns at 4.2 GHz are shown in Figure 8. Resonant arms for the E-Field are located on the vertical side of the design, whereas resonant arms for the H-Field are

concentrated on the horizontal side. Resonant arms with low currents are designated as blue, whereas those with high currents are shown in red.

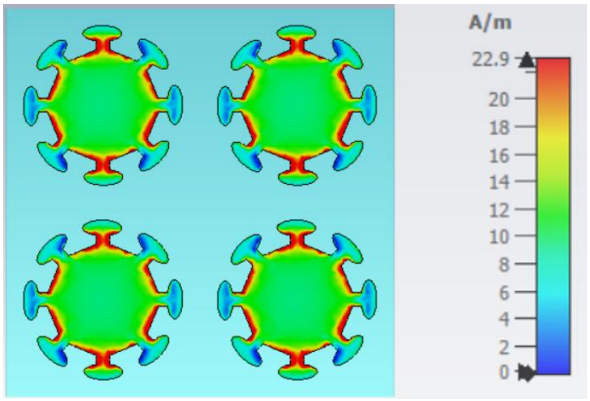

Figure 8. Surface current distribution of proposed FSS design.

The reflection phase of the proposed FSS configuration is shown in Figure 9. Because the unit cell is designed symmetrically, it is critical to investigate how the reflection phase changes with polarization. To validate this, an electromagnetic wave orientated along the x-axis is incident on the FSS surface while all other parameters are held constant, and the observed result is presented at 4.2 GHz. Similarly, the reflection phase plot of a y-polarized electromagnetic pulse has been investigated in both bands. Despite the fact that it is divided into phases, the layout remains consistent.

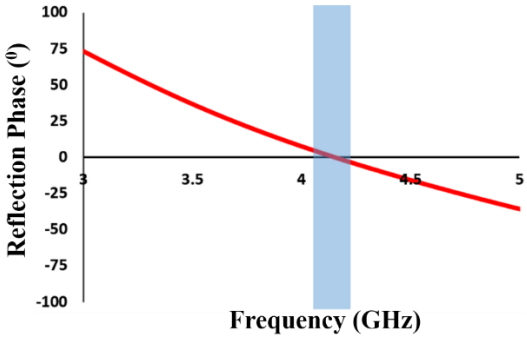

Figure 9. Simulated reflection phases of the proposed design at 4.2 GHz.

An Agilent Vector Network Analyzer (VNA), which evaluates parameters including bandwidth and reflection coefficients, is used to assess the operation of the manufactured design. Figure 10 displays a picture of the produced prototype that presentss both transparency and adaptability. It is evident that the investigated FSS structure offers their flexibility and transparency given in Figure 10(a) and 10(b). Moreover, to analysis the strength of the porposed design, the transparency, flexibility and mechanical properties of the acrylic substrate is given in Table 1 and Table 2, respectively.

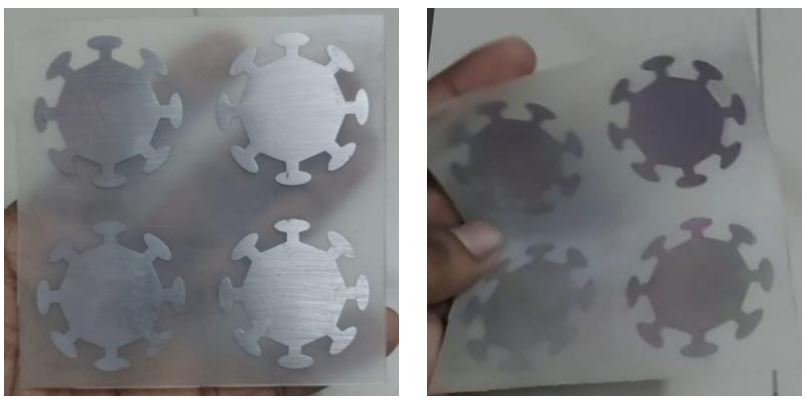

(a) (b)

Figure 10. Fabricated Prototype of the proposed FSS. (a) Transparency and (b) Flexibility.

Table 1. Transparency Properties of the proposed FSS design

Property	Value	Units	Standard/Notes
Light Transmission	92-94%	%	Visible spectrum (400-700 nm)
Opacity	6-8%	%	(100% - Transmission)
Haze	<1%	%	ASTM D1003
Refractive Index	1.49	-	At 589 nm (sodium D-line)
Clarity Rating	Excellent	-	Optical grade classification

Table 2. Flexibility/Mechanical Properties of the proposed FSS design

Property	Value	Units	Standard/Notes
Young's Modulus (Tensile)	3.2 GPa	GPa	ASTM D638
Young's Modulus (Imperial)	464,000 psi	psi	0.46×10^6 psi
Flexural Modulus	3.1-3.3 GPa	GPa	ASTM D790
Shear Modulus	1.7 GPa	GPa	-
Flexibility Classification	Semi-Flexible	-	Rigid plastic category

Figure 11 displays the resulting reflection value of the proposed FSS's noticed and computed curves. The S_{11} parameter stays constant when being used in measurements, as the graph makes clearly. The simulation shows that this FSS resonates around 4.2 GHz, while the measured impedance bandwidth at level S_{11} < -10 dB is approximately 1 GHz (3.6 – 4.6 GHz) and 710 MHz (4.1 – 4.8 GHz). The results of the simulation and the fabrication show good agreement. The measurement tolerance could be the cause of the little fluctuation in the reflection coefficient seen in the resonance frequency.

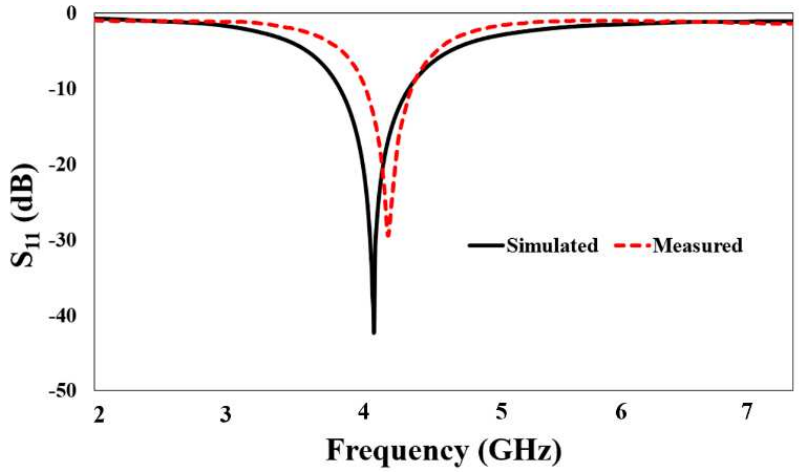

Figure 11. The combined simulated and measured reflection coefficient.

Table 3 contrasts the recommended FSS design with the compact, stable FSSs that are currently in use and are described in the short literature based on their stability, size, and operation frequency. The developed FSS structure presents notable improvements in both size reduction and stability capabilities compared to earlier reported designs. Featuring a compact unit cell of 11 × 11 × 1 mm, the design delivers performance on par with or exceeding that of larger counterparts, while operating at an elevated frequency of 4.2 GHz. The selection of acrylic as the substrate material enables a rare combination of optical transparency and mechanical flexibility, setting this work apart from prior studies [17–25]. While earlier efforts have demonstrated either flexible designs [17, 18, 20, 21] or transparent configurations [19], the integration of both characteristics in a single FSS design appears to be achieved here for the first time. The angular stability of 45°, though somewhat lower than that of certain rigid designs [18, 19, 22–25], is consistent with the performance of flexible alternatives [20, 21], and is a reasonable compromise considering the added functionality. With an operating frequency situated at 4.2 GHz, the design fits well within the spectrum of existing FSS technologies and outperforms bulkier configurations such as those measuring 26 × 26 × 1.6 mm [19, 24] in terms of miniaturization. The reduced footprint and innovative material choice mark a significant step forward in the realization of transparent, flexible components suitable for emerging wireless communication applications.

Table 3. Comparison with previously published FSS structures.

Reference no.	Unitcell size (mm)	Substrate used	Operating frequencies (GHz)	Stability	Properties
This Work	**11×11×1**	**Acrylic**	**4.2**	**45**	**Transparent & Flexible**
[17]	6×6×0.12	PET	3.5	60	Flexible & Reconfigurable
[18]	7.5×7.5×1.8	Plastic (ε_r = 3.2)	12.5	60	Transparent & Flexible
[19]	26×26×1.6	Float glass	0.85, 1.9 & 2.4	80	Transparent
[20]	10×10	Polyimide	9.81 & 11.61	45	Flexible
[21]	10×10×0.1	RT/duroid 5880	10	60	Flexible
[22]	9.45×9.45	Rogers 4350	2.4	80	-
[23]	7×7×0.78	RT/duroid 5880	7.9 & 11.9	75	-
[24]	26×26×1.6	FR-4	0.85, 1.9 & 2.4	60	-
[25]	18×18×1.6	FR-4	2.55, 3.5 & 5.6	75	-

5. CONCLUSION

The proposed modified octagonal-shaped FSS performs well for 5G communication at frequencies below 6 GHz. The compact size (11 x 11 × 1 mm³), angular stability up to 45°, and structural design allow for independent control of the passband and stopband, making it technically superior to many traditional FSS arrangements. Furthermore, the structure provides greater transparency and versatility, making it ideal for integration into current, space-constrained wireless systems. These qualities not only help to increase electromagnetic performance, but they also show a high potential for practical application in sophisticated 5G and satellite communication systems. The demonstrated flexibility and robustness of this design make it an attractive choice for future high-performance communication networks. Only PMMA (acrylic) substrates were used in this investigation, which limited its applicability to other transparent flexible materials like polycarbonate or polyethylene terephthalate (PET). The creation of advanced FSS designs with angular stability up to 75° for both TE and TM modes, possibly through miniature designs, that are able to function steadily at incident angles that are close to 90°.

FUNDING INFORMATION

There is no funding involved.

AUTHOR CONTRIBUTIONS STATEMENT

Name of Author	C	M	So	Va	Fo	I	R	D	O	E	Vi	Su	P	Fu
Gotte Ranjith Kumar	✓	✓	✓	✓	✓	✓		✓	✓				✓	
Swetha. S		✓	✓		✓	✓	✓	✓	✓		✓		✓	
Deepan. S		✓	✓	✓			✓		✓		✓			
Loganathan. AS		✓		✓	✓	✓	✓		✓	✓		✓		✓
Muthu Manickam. A		✓		✓	✓	✓		✓		✓		✓		✓
Anita Daniel. D	✓	✓		✓	✓	✓		✓		✓			✓	✓

C : **C**onceptualization
M : **M**ethodology
So : **So**ftware
Va : **Va**lidation
Fo : **Fo**rmal analysis
I : **I**nvestigation
R : **R**esources
D : **D**ata Curation
O : Writing - **O**riginal Draft
E : Writing - Review & **E**diting
Vi : **Vi**sualization
Su : **Su**pervision
P : **P**roject administration
Fu : **Fu**nding acquisition

CONFLICT OF INTEREST STATEMENT

Authors state no conflict of interest.

DATA AVAILABILITY

The authors confirm that the data supporting the findings of this study are available within the article and its supplementary materials.

REFERENCES

[1] F. Yang and Y. Rahmat-Samii, Electromagnetic Band Gap Structures in Antenna Engineering. Cambridge, U.K.: Cambridge Univ. Press, 2009.

[2] Q. Bai, K. L. Ford, and R. J. Langley, "Switchable electromagnetic bandgap surface wave antenna," Int. J. Antennas Propag., vol. 2014, Art. ID 693852, pp. 1–7, 2014.
[3] N. Kushwaha and R. Kumar, "Study of different shape Electromagnetic Bandgap (EBG) structures for single and dual band applications," J. Microw. Optoelectron. Electromagn. Appl., vol. 13, pp. 16–30, 2014.
[4] C. Huang, C. Ji, X. Wu, J. Song, and X. Luo, "Combining FSS and EBG surfaces for high-efficiency transmission and low-scattering properties," IEEE Trans. Antennas Propag., vol. 66, no. 3, pp. 1628–1632, Mar. 2018.
[5] G. Gao, S. Wang, R. Zhang, C. Yang, and B. Hu, "Flexible FSS-backed PIFA based on conductive textile and PDMS for wearable applications," Microw. Opt. Technol. Lett., vol. 62, no. 4, pp. 1733–1741, Apr. 2020.
[6] A.Y. Ashyap et al., "Highly efficient wearable CPW antenna enabled by FSS-FSS structure for medical body area network applications," IEEE Access, vol. 6, pp. 77529–77541, 2018.
[7] B. Mustafa and T. Rajendran, "Wearable multilayer patch antenna with electromagnetic band gap structure for public safety systems," IETE J. Res., vol. 68, no. 4, pp. 2979–2988, 2022.
[8] Y. J. Lee, J. Yeo, R. Mittra, and W. S. Park, "Design of a high-directivity electromagnetic band gap (FSS) resonator antenna using a frequency-selective surface (FSS) superstrate," Microw. Opt. Technol. Lett., vol. 43, no. 6, pp. 462–467, Jun. 2004.
[9] S. Chaimool, C. Rakluea, and P. Akkaraekthalin, "Compact wideband microstrip thinned array antenna using FSS superstrate," AEU-Int. J. Electron. Commun., vol. 66, no. 1, pp. 49–53, 2012.
[10] A.A. Althuwayb et al., "Metasurface-inspired flexible wearable MIMO antenna array for wireless body area network applications and biomedical telemetry devices," IEEE Access, vol. 11, pp. 1039–1056, 2023.
[11] N. P. Kulkarni, N. B. Bahadure, P. D. Patil, and J. S. Kulkarni, "Flexible interconnected 4-port MIMO antenna for sub-6 GHz 5G and X band applications," AEU-Int. J. Electron. Commun., vol. 152, p. 154243, 2022.
[12] M. D. Geyikoglu, "A novel UWB flexible antenna with dual notch bands for wearable biomedical devices," Analog Integr. Circ. Sig. Process., vol. 114, pp. 439–450, 2023.
[13] M. Al-Hasan et al., "Metamaterial inspired electromagnetic bandgap filter for ultra-wide stopband screening devices of electromagnetic interference," Sci. Rep., vol. 13, no. 1, p. 13347, 2023.
[14] T. H. Dam, M. T. Le, Q. C. Nguyen, and T. T. Nguyen, "Dual-band metamaterial-based FSS antenna for wearable wireless devices," Int. J. RF Microw. Comput. Aided Eng., vol. 2023, Art. ID 2232674, pp. 1–11, 2023.
[15] K. S. Parvathi and S. R. Gupta, "Novel dual-band FSS structure to reduce mutual coupling of air gap-based MIMO antenna for 5G application," AEU-Int. J. Electron. Commun., vol. 138, p. 153902, 2021.
[16] S. Karamzadeh and V. Rafiei, "Dual-band antenna modification by using dual band FSS structure for WLAN/WiMAX applications," J. Instrum., vol. 15, no. 4, p. P04025, 2020.
[17] T. Tian et al., "Flexible and reconfigurable frequency selective surface with wide angular stability fabricated with additive manufacturing procedure," IEEE Antennas Wireless Propag. Lett., vol. 19, no. 12, pp. 2428–2432, Dec. 2020.
[18] A. Dewani, S. G. O'Keefe, D. V. Thiel, and A. Galehdar, "Optically transparent frequency selective surfaces on flexible thin plastic substrates," AIP Adv., vol. 5, no. 2, 2015.
[19] H. Zhu, S. Jin, and J. Shao, "Transparent and angular stably miniaturized frequency selective surface for tri-band GSM shielding," IEICE Electron. Exp., vol. 21, no. 22, p. 20240485, 2024.
[20] N. Prasad et al., "Flexible metamaterial-based frequency selective surface with square and circular split ring resonators combinations for X-band applications," Mathematics, vol. 11, no. 4, p. 800, 2023.
[21] M. Bilal et al., "Miniaturized and flexible FSS-based EM shields for conformal applications," IEEE Trans. Electromagn. Compat., vol. 62, no. 5, pp. 1703–1710, 2020.
[22] M. Qu, B. Li, S. Sun, and S. Li, "Angularly stable bandpass frequency selective surface based on metasurface," IEEE Access, vol. 8, pp. 41684–41689, 2020.
[23] M. Idrees, Y. He, S. Ullah, and S. W. Wong, "A dual-band polarization-insensitive frequency selective surface for electromagnetic shielding applications," Sensors, vol. 24, no. 11, p. 3333, 2024.
[24] T. S. Kumar and K. J. Vinoy, "A miniaturized angularly stable FSS for shielding GSM 0.9, 1.8, and Wi-Fi 2.4 GHz bands," IEEE Trans. Electromagn. Compat., vol. 63, no. 5, pp. 1605–1608, 2021.
[25] J. Garg, S. Yadav, and M. M. Sharma, "A novel miniaturized loop-based angularly stable and polarization-independent multiband bandpass FSS structure for Wi-Max and WLAN applications," Sādhanā, vol. 48, no. 1, p. 14, 2023.

BIOGRAPHIES OF AUTHORS

Gotte Ranjithkumar is a scholar in Jawaharlal Nehru Technological University, Hyderabad, Telangana, India, received a B.Tech degree in Computer Science and Information Technology in 2006 from Kamala Institute of Technology and Science,Singapur,Karimnagar, Telangana, India, affiliated to JNTU Hyderabad, and a M.Tech degree in Software Engineering specialization in 2009 from Kakatiya Institute of Technology and Science,warangal, Telangana, India, affiliated to Kakatiya University,Warangal, Telangana, India. Currently working as assistant professor in SR University,Warangal, Telangana, India. His interested research areas include deep learning, Blockchain Technology & Cyber security.

Swetha. S was born on 4th May 1989 in Madurai, Tamil Nadu, India. She received her Bachelor's degree in Electronics and Communication Engineering from Mohammed Sathak Engineering College, kilakarai in 2010, Master's degree in Embedded systems from Karunya University, Coimbatore in 2012. She is currently an Assistant Professor in the Department of Electronics and Communication Engineering at St. Joseph's Institute of Technology, Chennai. She has more than 5 years' experience in teaching. Her research interests include Embedded systems, Machine Learning, wireless communication and microwave design.

Deepan. S is an Assistant professor and researcher in the field of computer science and engineering. He completed his Bachelor of Technology (B.Tech) in Information Technology from Valliammai Engineering College in 2007. Later, he pursued a Master of Technology (M.Tech) in Computer Science Engineering in 2015 from SRM Institute of Science and Technology, Kattankulathur, Tamil Nadu, India. Currently, he is pursuing his Doctoral studies (Ph.D.) at the Department of Networking and Communications, College of Engineering and Technology, SRM Institute of Science and Technology, Kattankulathur. His research interests lie in the areas of antennas, Machine Learning, Internet of Things (IoT), and Deep Learning.

Loganathan. AS was born on 15th June 1985 in Chennai, Tamilnadu, India. He received his Bachelor's degree in Electronics and Communication Engineering from S.A.Engineering College, Anna University, Chennai in 2006, Master's degree in VLSI Design from Sathyabama University, Chennai in 2012. He is currently an Assistant Professor in the Department of Electronics and Communication Engineering at Chennai Institute of Technology, Chennai. He has more than 11 years' experience in teaching. His research interests include Internet of Things, Low Power VLSI design and Microwave.

MUTHU MANICKAM. A was born on 4th September 1979 in Thiruppathur, Tamilnadu, India. He completed his Bachelor's degree in Electronics and Communication Engineering from Mohamed Sathak Engineering College, Madurai Kamaraj University, Madurai in the year 2001. In continuous, he completed his M.E. degree in Communication Systems from K.L.N College of Engineering, Anna University, Chennai in the year 2007. As a golden achievement, he has completed his Ph.D. award in the field of RF and Antenna from K.L.N College of Engineering, Anna University Chennai in the year May 2022. He is an active and executive committee member in various professional bodies like IEI, ISTE, CSI, IETE, ORSI, OSI, CRSI and CSTA. His research interests include Antenna, Optical Communication and MIMO systems.

Lavanya. S received her Bachelor's degree in Electronics and Communication Engineering from SSN College of Engineering ,Chennai, Tamil Nadu, India in 2002. She received Master's degree in Applied Electronics in Sathyabama University, Chennai, Tamil Nadu, India in 2012 doing Ph.D. in Anna University,Chennai, Tamil Nadu, India. She is currently working as an Assistant Professor in the Department of Biomedical Engineering, Jerusalem College of Engineering , Chennai, Tamil Nadu, India. Her major areas of interest are Wireless communication , Embedded systems and Digital signal Processing .